Supporting Information

Ferrara et al. 10.1073/pnas.1108455108

SI Methods

Production of Unmodified and Afucosylated IgGs. Unmodified (wild-type) antibodies, expressed in CHO cells, bear carbohydrates attached to the Fc fragment that are mainly biantennary, fucosylated (97%) with a variable galactose content (Fig. S1 and Fig. 1*B*). Afucosylated (83%) antibodies were produced in a cell line overexpressing β1,4-N-acetylglucosaminyltransferase III (GnT-III), an enzyme catalyzing the addition of a bisecting GlcNAc to the β-mannose of the core (Fig. S1 and Fig. 1*B*). By adding a bisecting GlcNAc the action of α1,6 core fucosyltransferase is blocked during antibody biosynthesis (1).

Oligosaccharide Analysis. Human IgG1 and FcγRIIIa variants were treated with sialidase (QA-Bio) following the manufacturer's instructions prior to PNGase F digestion. The neutral oligosaccharides of hIgG1 were obtained by PNGase F (QA-Bio) digestion as previously described (1). For the oligosaccharide profiling of FcγRIIIa variants, the protein was reduced and alkylated in solution prior to sialidase and PNGase F digestion (adapted from ref. 2). The carbohydrate profiles were analyzed by mass spectrometry (Autoflex, Bruker Daltonics GmbH) in positive ion mode as previously described (1).

Surface Plasmon Resonance. The surface plasmon resonance (SPR) experiments were performed on a BIACORE T100 at 25 °C with HBS-EP (0.01 M Hepes pH 7.4, 0.15 M NaCl, 3 mM EDTA, 0.005% surfactant P20) as running buffer. The capturing agent (anti-human Fab, GE Healthcare) was immobilized on all four flow cells of a CM5 chip (GE Healthcare) at 8,000–9,000 RU using a standard amine coupling procedure. Fucosylated and afucosylated antibodies were injected on flow cell two and three for 90 s with a flow rate of 30 μL min^{-1}, respectively. After a stabilization period of 15 s, the Fcγ receptor variant (FcγRIIIa, FcγRIIIa-N45N162 or -N45N162-kif) was injected for 180 s at various concentrations (from 0.98 to 4,000 nM) with a flow rate of 50 μL min^{-1} on all flow cells. The dissociation phase was monitored for 220 s. The chip surface was regenerated after every cycle using a triple injection of 60 s 10 mM glycine-HCl pH 2.1. Bulk refractive index differences were corrected by subtracting the response obtained on the reference flow cell. Binding kinetics were analyzed by BiaEvaluation software (GE Healthcare) using a 1:1 Langmuir binding model. All injections were carried out in duplicate. Only one of the duplicates is shown. For some of these interactions, featuring too fast dissociation to allow the determination of kinetic constants, the affinity constant K_D was determined by steady state analysis.

Antibody-Dependent Cellular Cytotoxicity (ADCC) Assay. The cytotoxic potential of the antibodies was assessed as previously described (1). Briefly, CD20-positive Z-138 cells (RPMI medium 1640, 10% FCS, 1% glutamax, Invitrogen AG) labeled with calcein AM were used as target cells. Serial dilutions of antibodies were incubated with the target cells for 10 min at room temperature prior to the addition of effector cells [peripheral blood mononuclear cells (PBMCs) from a donor homozygous for FcγRIIIa-V158] with effector to target ratio of 25:1. Calcein release was assessed as previously described (1). Specific lysis was calculated relative to the total lysis control, resulting from incubating the target cells with 1% Triton X-100. Percentage of specific antibody-mediated killing was calculated as previously described (1). Each antibody dilution was analyzed in triplicate.

B-Cell Depletion in Whole Blood Assay. Heparinized blood (280 μL) from a healthy FcγRIIIa-V158 homozygous donor was incubated at 37 °C with 20 μL PBS or 15-fold concentrated antibody glycovariants (final concentrations of 0.01, 0.06, 0.3, 2, 8, 40, 200, 1,000 ng/mL). After 24 h, 35 μL of blood was stained with a mixture of anti-CD19-PE, anti-CD3-FITC, and anti-CD45-CyChrome (BD Biosciences) for 15 min at room temperature. Before analysis, 200 μL of BD FACS lysis solution (BD Biosciences) was added. The CD3-FITC and CD19-PE fluorescence of the blood samples was flow cytometrically analyzed by gating on all CD45-positive cells. B-cell depletion was determined by plotting the ratio of CD19-positive B cells to CD3-positive T cells. Each antibody concentration was analyzed in triplicate.

Protein Data Bank (PDB) Search for Carbohydrate–Carbohydrate Interactions within Protein Complexes. We performed an extensive search throughout the PDB to identify existing structures with a carbohydrate–carbohydrate interface within protein–protein complexes. Out of roughly 1,500 entries containing carbohydrates, we could select around 250 entries representing protein complexes. Within these entries we were not able to identify any protein complex with a carbohydrate–carbohydrate interface.

1. Ferrara C et al. (2006) Modulation of therapeutic antibody effector functions by glycosylation engineering: Influence of Golgi enzyme localization domain and co-expression of heterologous beta1, 4-N-acetylglucosaminyltransferase III and Golgi alpha-mannosidase II. *Biotech Bioeng* 93:851–861.

2. Papac DI, Briggs JB, Chin ET, Jones AJ (1998) A high-throughput microscale method to release N-linked oligosaccharides from glycoproteins for matrix-assisted laser desorption/ionization time-of-flight mass spectrometric analysis. *Glycobiology* 8:445–454.

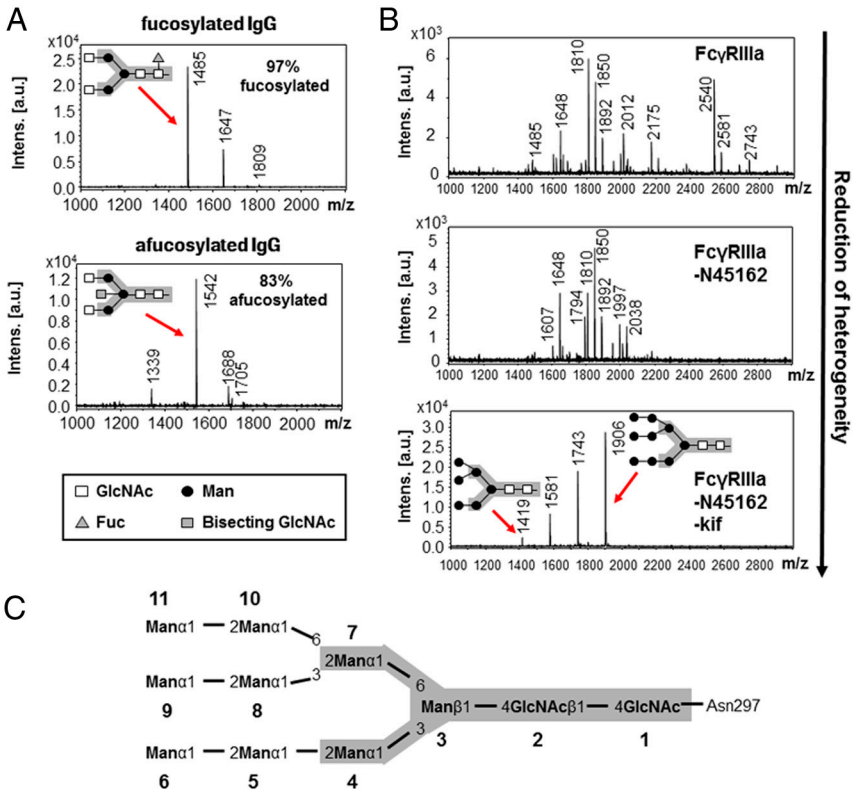

Fig. S1. Reduction of FcγRIIIa's carbohydrate heterogeneity and oligosaccharide profiles of IgG1s. (*a*) MALDI-TOF MS spectra analyzed in positive ion mode of oligosaccharides released from human IgG1 variants by sialidase and PNGaseF digestion. (*b*) MALDI-TOF MS spectra analyzed in positive ion mode of oligosaccharides released from FcγRIIIa variants by sialidase and PNGaseF digestion. (*c*) High mannose type oligosaccharides found on FcγRIIIa expressed in the presence of kifunensine. GlcNAc, N-acetylglucosamine; Fuc, fucose; Man, mannose; kif, kifunensine.

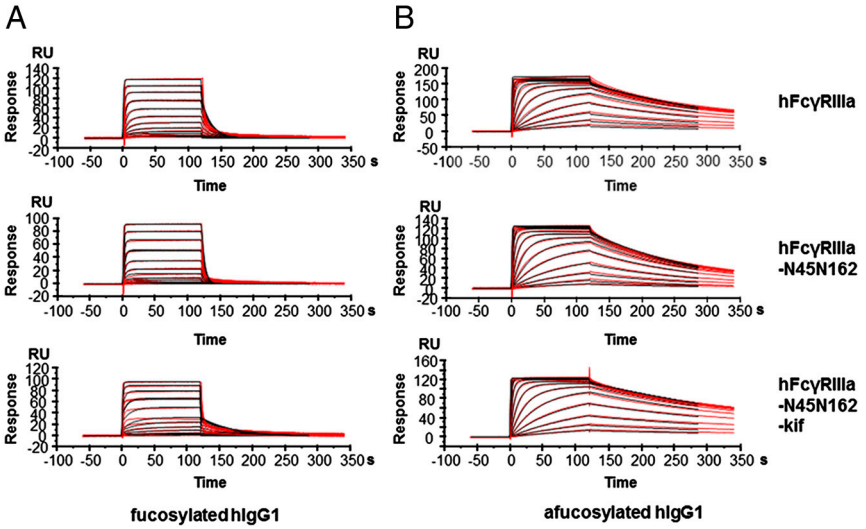

Fig. S2. Fittings of the interaction between FcγRIIIa variants and hIgG1 glycoforms. Fittings for the interactions of FcγRIIIa variants injected at different concentrations (from 0.98 to 4,000 nM) on captured (*a*) fucosylated hIgG1 or (*b*) afucosylated hIgG1. Binding kinetics were evaluated using a 1:1 Langmuir binding model; binding constants are summarized in Table 1. For some of these interactions, featuring too fast dissociation to allow the determination of kinetic constants, the affinity constant K_D was determined by steady state analysis.

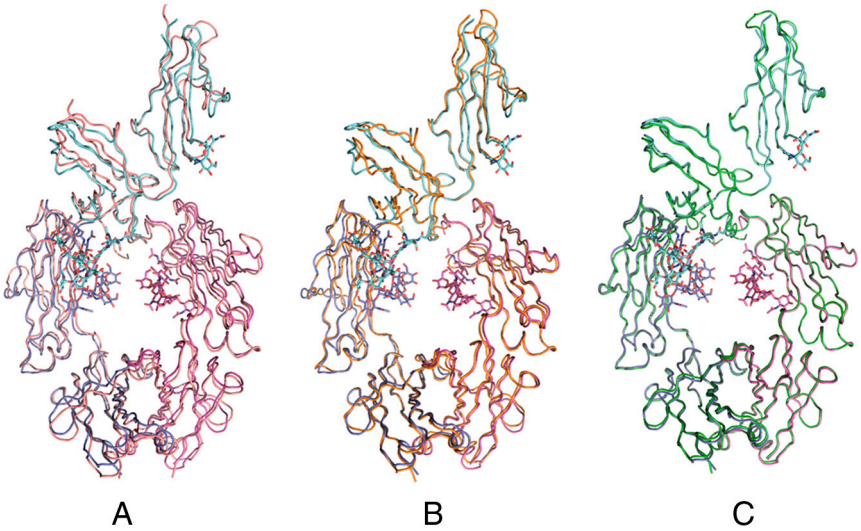

Fig. S3. Overlay of the afucosylated Fc-FcγRIIIa complex with fucosylated Fc-FcγRIIIa (*c*) or previously published structures (*a* and *b*) of aglycosylated FcγRIIIb complexed to fucosylated Fc. (*a*) Overlay with coordinates of PDB ID code 1E4K (1) shown in magenta, (*b*) with PDB ID code 1T83 (2) shown in red, and (*c*) with fucosylated Fc-FcγIIIa (shown in green). Only the glycosylation trees of the afucosylated Fc complex are depicted in ball and stick.

1. Sondermann P, Huber R, Oosthuizen V, Jacob U (2000) The 3.2-A crystal structure of the human IgG1 Fc fragment-Fc gammaRIII complex. *Nature* 406:267–273.
2. Radaev S, Motyka S, Fridman WH, Sautes-Fridman C, Sun PD (2001) The structure of a human type III Fcgamma receptor in complex with Fc. *J Biol Chem* 276:16469–16477.

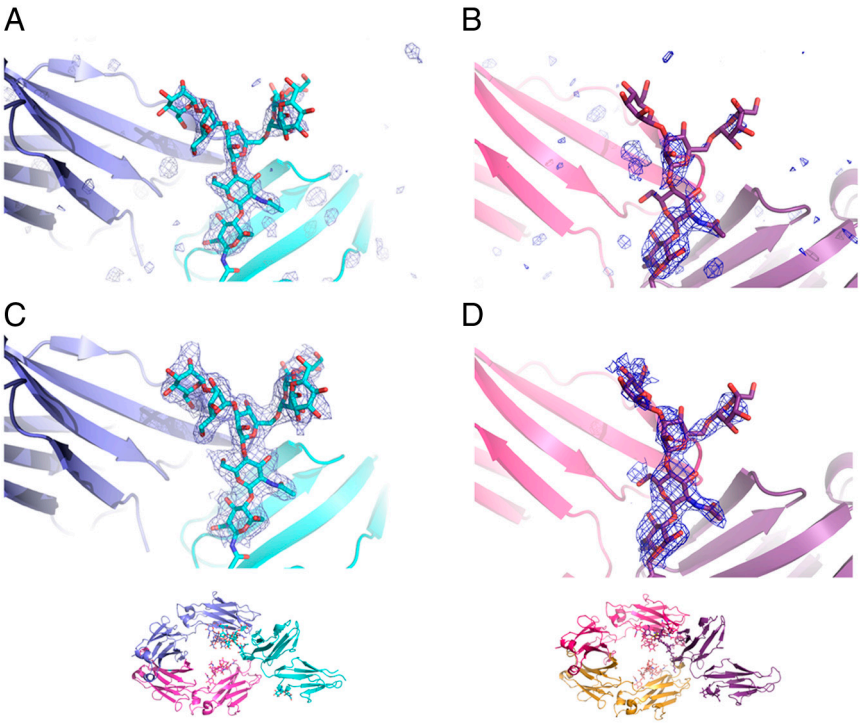

Fig. S4. We calculated a Fo-Fc electron density map after molecular replacement (contoured at 3σ) and a 2Fo-Fc electron density map after the refinement process (contoured at 1σ). The area around the N-linked glycosylation site at Asn162 is shown. As reflected by the quality of the map, the receptor carbohydrate at Asn162 when complexed to afucosylated Fc is much better defined compared to the corresponding carbohydrate of the receptor in complex with fucosylated Fc. (*a*) Fo-Fc electron density map for the afucosylated Fc-FcγRIIIa structure. The Fc heavy chain is shown in blue, the receptor in cyan. (*b*) Fo-Fc electron density map for the complex with fucosylated Fc (magenta). The receptor is colored in dark violet. (*c*) 2Fo-Fc electron density map for the afucosylated Fc-FcγRIIIa structure and (*d*) for the complex with fucosylated Fc. The carbohydrate at Asn162 is depicted in both pictures as ball and stick. The carbohydrates of the Fc chain are not shown.

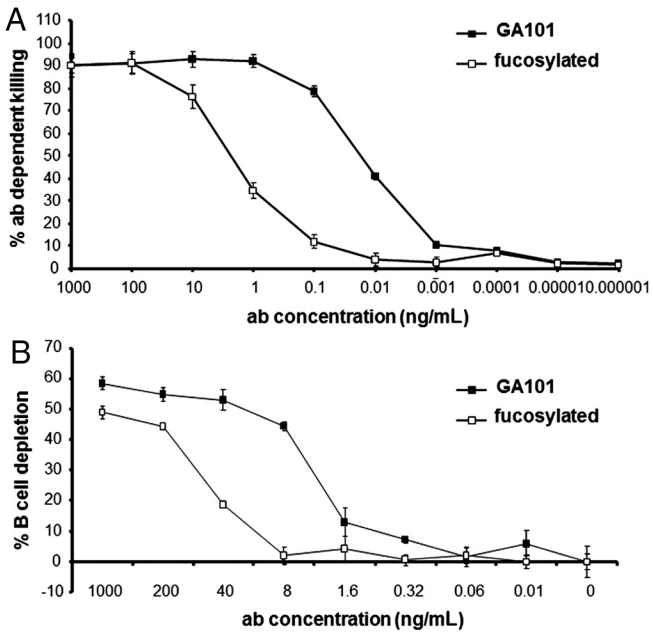

Fig. S5. Biological activity of anti-CD20 GA101. (*a*) ADCC using PBMCs (FcγRIIIa-V158 homozygous) as effectors and human lymphoma Z138 dells as targets. (*b*) B-cell depletion in whole blood (FcγRIIIA-V158 homozygous), which was calculated from the ratio of CD19-positive B cells to CD3-positive T cells as measured by FACS analysis. Filled squares, GA101; open squares, fucosylated variant.

Table S1. Effect of removal of N-linked glycosylation sites in FcγRIIIa on its expression

Mutant	Asn38	Asn45	Asn74	Asn162	Asn169	Expression
Wild type	Asn	Asn	Asn	Asn	Asn	++++
1	Asn	Asn		Asn		+++
2	Asn		Asn	Asn		+
3	Asn			Asn		+
4				Asn	Asn	+
5			Asn	Asn		+
6		Asn		Asn		++
7				Asn		-

Sites were deleted by exchange of the Asn to a Gln residue.

Table S2. Data collection and refinement statistics

	Crystal afucosylated	Crystal fucosylated
Data collection		
Space group	$P2_12_12_1$	$P2_12_12_1$
Cell dimensions		
a, *b*, *c*, Å	67.3, 88.2, 141.1	67.7, 88.5, 140.3
α, β, γ, °	90, 90, 90	90, 90, 90
Resolution, Å	2.36 (2.45–2.36)*	2.2 (2.25–2.20)*
R_{sym}	0.072 (0.75)	0.126 (0.76)
$I/\sigma I$	12.56 (1.31)	10.28 (1.4)
Completeness, %	99.9 (99.9)	100.0 (100.0)
Redundancy	6.63 (6.82)	6.84 (6.71)
Refinement		
Resolution, Å	50–2.4	50–2.2
No. reflections	31,967	40,758
R_{work}/R_{free}	20.5/24.9	19.4/25.2
No. atoms		
Protein	4,688	4,831
Oligosaccharide	328	299
Water	140	321
B factors		
Protein	37.94	30.00
Oligosaccharide	53.04	54.33
Water	55.03	44.75
rms deviations		
Bond lengths, Å	0.009	0.011
Bond angles, °	1.453	1.67
Ramachandran statistics		
Most favored, %	93.4	92.6
Additional allowed, %	6.4	7.4
Disallowed, %	0.2	0.0
PDB ID code	3SGK	3SGJ

Number of crystals for each structure is one.
*Values in parentheses are for highest-resolution shell.

Table S3. Comparison of observed distances determined with COOT for the sugar–sugar interactions between N-linked glycosylation tree at Asn162 of the receptor and at Asn297 of chain A of Fc

hFcγRIIIa Asn162	Fc afuco Asn297	Distance in Å
GlcNAc1 O3	GlcNAc1 O7	2.8
GlcNAc2 O6	GlcNAc1 O6	2.7
	GlcNAc1 O5	3.2
Man5 O6	Gln295	2.5
Man7 O5	Tyr296	4.2
hFcγRIIIa Asn162	Fc wt-fuco Asn297	
GlcNAc1 O3	GlcNAc1 O7	3.3
GlcNAc2 O6	GlcNAc1 O6	4.2
	GlcNAc1 O5	4.3
	Fuc O5	2.9
Man5 O6	Gln295	Man not defined
Man7 O5	Tyr296	4.8